Materials Chemistry and Physics 221 (2019) 295–300

Contents lists available at ScienceDirect

Materials Chemistry and Physics

journal homepage: www.elsevier.com/locate/matchemphys

# [1]Benzothieno[3,2-*b*]benzothiophene (BTBT) derivatives: Influence in the molecular orientation and charge delocalization dynamics

Ana Buzzi Fernández[a,*], Amanda Garcez da Veiga[a], Almaz Aliev[b], Christian Ruzié[b], Guillaume Garbay[b], Basab Chattopadhyay[b], Alan R. Kennedy[c], Yves H. Geerts[b], Maria Luiza M. Rocco[a]

[a] Institute of Chemistry, Federal University of Rio de Janeiro, Rio de Janeiro, 21941-909, Brazil
[b] Laboratoire de Chimie des Polymères, Faculté des Sciences, Université Libre de Bruxelles (ULB), CP 206/1 Boulevard du Triomphe, 1050, Bruxelles, Belgium
[c] Department of Pure and Applied Chemistry, University of Strathclyde, 295 Cathedral Street, Glasgow, G1 1XL, Scotland, UK

## HIGHLIGHTS

- Structure-property relationship are investigated for three BTBT derivatives.
- Ordering and molecular orientation show differences between surface and bulk.
- Alkyl chains of different sizes influence the charge transport properties.
- ditBu-BTBT has the highest molecular ordering and the lowest charge transfer time.

## GRAPHICAL ABSTRACT

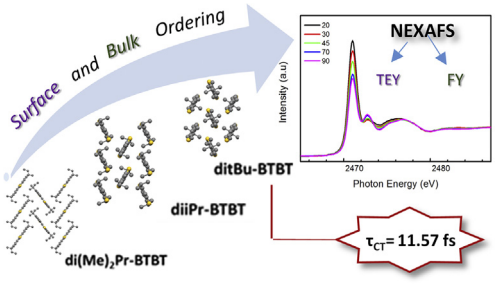


## ARTICLE INFO

*Keywords:*
Oligomers
Near-edge X-ray absorption fine structure
Charge transfer dynamics
Organic field effect transistors

## ABSTRACT

Using near-edge X-ray absorption fine structure (NEXAFS) and resonant Auger spectroscopy (RAS) in conjunction with the core-hole clock methodology the electronic structure, molecular ordering and orientation and charge transfer dynamics in the femtosecond time scale of 2,7-di-tert-pentyl[1]benzothieno[3,2-b]benzothiophene (di(Me)$_2$Pr-BTBT), 2,7-di-iso-propyl[1]benzothieno[3,2-b]benzothiophene (diiPr-BTBT) and 2,7-di-tert butyl[1]benzothieno[3,2-b]benzothiophene (ditBu-BTBT) films were investigated. Total electron yield (TEY) and fluorescence yield (FY) NEXAFS spectra were recorded with the aim of determining the preferred molecular orientation of the oligomers at the surface and in the bulk. Angular dependent sulfur 1s NEXAFS spectra for diiPr-BTBT and ditBu-BTBT films deposited onto FTO (fluorine doped tin oxide) point to well-organized films with a preferred edge-on geometry, while for the di(Me)$_2$Pr-BTBT film little variation is seen, indicating that the film matches its herringbone crystal packing. Films prepared on ITO (indium tin oxide) and silicon were also investigated by TEY and FY NEXAFS. Greater film ordering is observed in the bulk. The electron charge transfer time following sulfur K-edge main resonance was calculated. The ditBu-BTBT films showed the lowest charge transfer time as well as greater molecular organization, pointing to an increased coupling, as compared to the other oligomers.

* Corresponding author
*E-mail address:* buzzi@pos.iq.ufrj.br (A.B. Fernández).

https://doi.org/10.1016/j.matchemphys.2018.09.064
Received 13 July 2018; Received in revised form 7 September 2018; Accepted 19 September 2018
Available online 21 September 2018

## 1. Introduction

The field of molecular semiconductors has been widely studied due to the promising optoelectronic properties that are offered for the construction of organic photovoltaics, light emitting diodes and field effect transistors. Some of the advantages that they offer are low cost of production and deposition in flexible substrates. Currently several research groups dedicate their studies to the optimization of the structure of organic compounds for use in the construction of optoelectronic devices [1–5].

[1]benzothieno [3,2-b]benzothiophene (BTBT) derivatives are among the molecular semiconductors with mobility values of 10 $cm^2 V^{-1} s^{-1}$, or even higher, that are crucial for the construction of performing optoelectronic devices [6–9]. Other important characteristics to mention are the viability of its synthetic route and high chemical stability [6]. Different studies have shown that the fine tuning of molecular packing of the BTBT core allows a better understanding of the structure-property relationship [10,11]. Previous research has shown successful results for various derivatives of the BTBT core [12–15]. Also the addition of alkyl chains of different sizes is a way to adjust the charge transport properties [10,13].

The electronic structure, molecular ordering and orientation and charge transfer processes are important parameters that will affect charge mobility in organic semiconductors. The knowledge of these parameters is of great importance for the optimization of the structure to be used in the manufacture of devices [16] and therefore they were systematically pursued here. Three different BTBT derivatives, namely 2,7-di-tert-pentyl [1]benzothieno [3,2-b]benzothiophene (di(Me)$_2$Pr-BTBT), 2,7-di-iso-propyl [1]benzothieno [3,2-b]benzothiophene (diiPr-BTBT), and 2,7-di-tert butyl [1]benzothieno [3,2-b]benzothiophene (ditBu-BTBT), whose chemical structures are shown in Fig. 1, were studied aiming to gain further information on the structure-property relationship. ditBu-BTBT is the reference compound that shows the best charge transport [6]. The crystal structure of diiPr-BTBT is characterized by herringbone packing as for ditBu-BTBT but it exhibits a much greater structural disorder [6] that is anticipated to impact electronic properties. The crystal structure of di(Me)$_2$Pr-BTBT differs significantly from those of ditBu-BTBT and diiPr-BTBT. Aromatic core of di(Me)$_2$Pr-BTBT are much more separated from each other's. Intermolecular electronic interactions are expected to be considerably reduced (see Figs. 1 and 2).

Eletronic charge transfer times following sulfur K-edge were calculated by employing the so-called core-hole clock approach, a methodology that has been widely used for compounds containing thiophene units [1,2,17]. Photoabsorption spectroscopy (NEXAFS – near-edge X-ray absorption fine structure) allows the study of the unoccupied density of states, as well the analysis of the ordering and preferred molecular orientation at different depths of the films depending on the method of detection used [18,19]. NEXAFS spectra were obtained by detecting simultaneously the fluorescence yield (FY) and the total electron yield (TEY). Detection methods that involve the detection of electrons, such as TEY, depend on the inelastic mean free path of the electrons in the solid [20]. For tender X-ray photons, the sampling depth for TEY was estimated as being at least 40 nm [21]. On the other hand, the FY method involves the detection of photons that are much more energetic and penetrating. That is why this method offers information regarding the bulk of the films [20,22]. Films prepared on different substrates were also investigated by TEY and FY NEXAFS spectroscopy to learn about the influence of substrates in the morphology of the films.

## 2. Experimental

The diiPr-BTBT and ditBu-BTBT oligomers were synthesized according to previous publications [6]. The synthesis and characterization of di(Me)$_2$Pr-BTBT are given in supporting information.

### 2.1. Single crystal X-ray diffraction

X-ray diffraction data for crystals of compound di(Me)$_2$Pr-BTBT were collected at 123 K with graphite monochromated Cu Kα radiation (λ = 1.5418 Å) using an Oxford Diffraction Gemini S instrument. The displacement parameters of all non-H-atoms were treated anisotropically. H-atoms were placed at calculated positions using suitable riding models with isotropic thermal parameters $U_{iso}(H) = 1.2U_{eq}(C)$ for CH and $CH_2$ groups and $U_{iso}(H) = 1.5U_{eq}(C)$ for $CH_3$ groups. The crystal structure was solved by direct methods and refined by full matrix least-squares methods based on $F^2$ using the SHELXL-2014 program [23]. Crystal data is summarized in Table S1 and full details are available in CIF format.

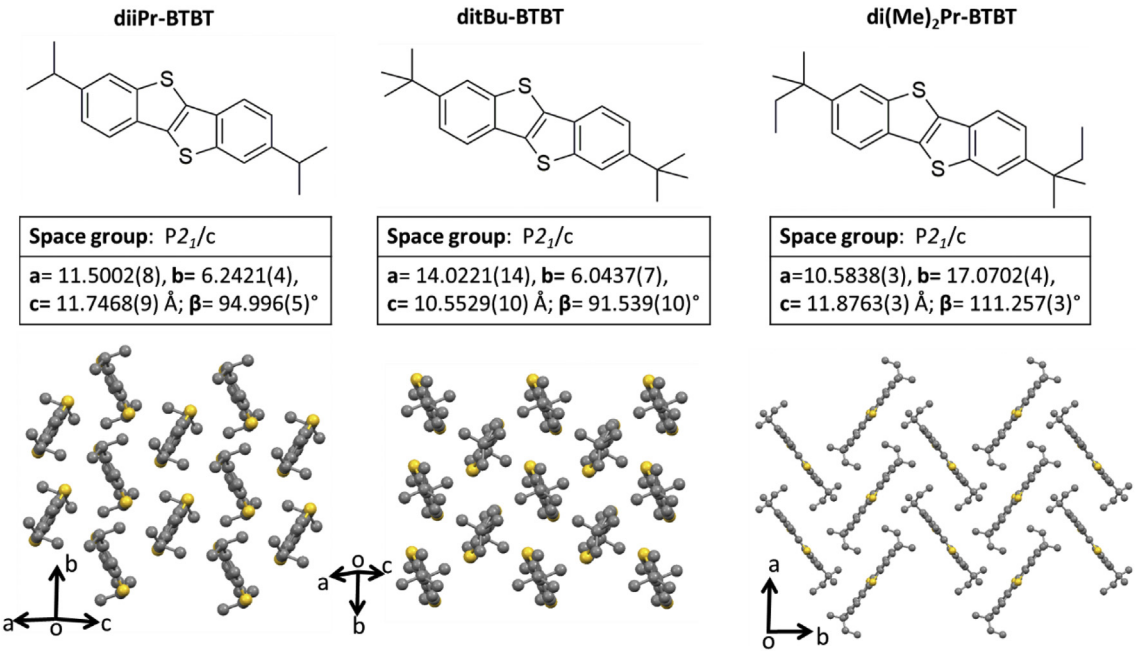


**Fig. 1.** Molecular and Crystal structure of compounds under study.

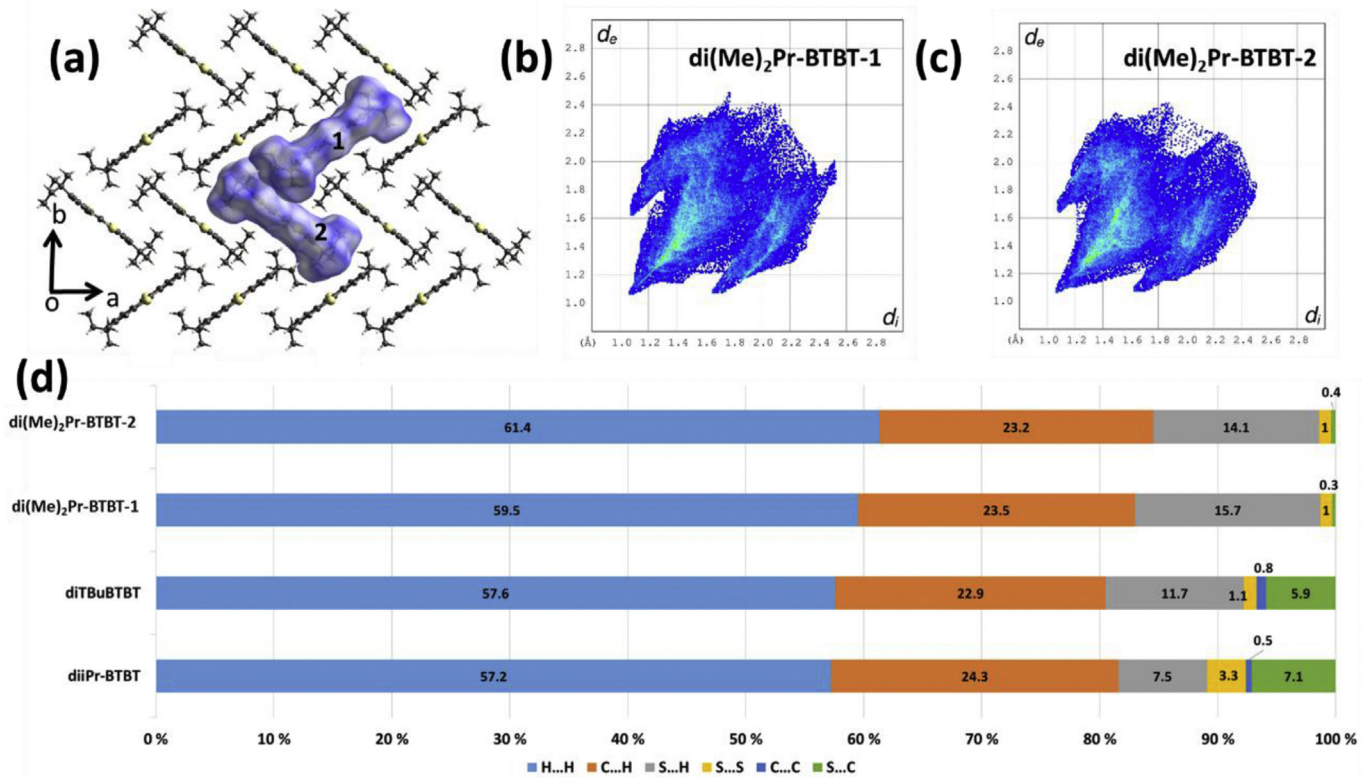


**Fig. 2.** (a) Hirshfeld surfaces and (b) and (c) relative fingerprint plots of the two molecules present in the asymmetric unit of di(Me)$_2$Pr-BTBT, mapped over a $d_{norm}$ range of −0.5 to 1.5 Å. (d) Percentage contributions to the Hirshfeld surface area for the various close intermolecular contacts.

Films of diiPr-BTBT, ditBu-BTBT and di(Me)$_2$Pr-BTBT were deposited by spin coating onto fluorine doped tin oxide (FTO) substrate in a nitrogen atmosphere, from 5 mg/mL chloroform solution. Film thickness of ~90 nm was measured using a Dektak 150 profilometer (Veeco Instruments) for all samples. The substrates were cleaned before thin film deposition by ultrasonic treatment in acetone and isopropanol for 15 min. Oligomers films were also deposited on Si and indium tin oxide (ITO) substrates for comparison, following the same deposition procedure.

NEXAFS and Auger decay measurements were conducted at the Brazilian Synchrotron Light Source (LNLS) at the soft X-ray spectroscopy (SXS) beamline. The Si(111) double-crystal monochromator, which covers sulfur K-edge and provides an energy resolution of 380 meV, was used. The well-established value of the $2p_{3/2} \rightarrow 4d$ transition for metallic molybdenum (2520 eV) [24] was taken for energy calibration. The polarization degree of the synchrotron radiation was > 0.95. Two different NEXAFS detection modes are compared under the same experimental condition: TEY and FY. TEY NEXAFS spectra were recorded by measuring simultaneously the current of an Au grid placed before the sample and the drain current at the sample. FY NEXAFS data were collected using a silicon drift detector. In order to correct any fluctuation of the beam, all spectra were normalized by the photon flux from the gold grid. NEXAFS spectra were measured by varying the angle of incidence of the synchrotron radiation for dichroism studies.

Auger decay spectra were obtained using a hemispherical electron energy analyzer at 20 eV of pass energy, which was mounted in a UHV chamber with a base pressure of $10^{-8}$ mbar. During the measurements the angle between the substrate and the analyzer was set to 45°. Shirley function was used for subtraction of the spectral background in a range of kinetic energy of 2100–2125 eV. A linear combination of Gaussian and Lorentzian functions (a pseudo Voight line shape profile) with a mixing factor of GL (50) was employed for deconvoluting the Auger spectra, using the CasaXPS software. Full width at half maximum (FWHM) was fixed at the same value for the same type of Auger decay channel (spectator or normal) in both spectra [17,25,26]. The spectra were calibrated in energy using 2900 eV photon energy and the well-known photoemission line of the Au $4f_{7/2}$ (84 eV) line [27,28].

## 3. Results and discussion

Crystal structure determination for di(Me)$_2$Pr-BTBT was realized from single crystal diffraction data, the corresponding crystal data are given in Table S1. For diiPr-BTBT and ditBu-BTBT, the crystal structures have already been reported [6]. A comparative view of the molecular and the crystal structure of the compounds are given in Fig. 1. All the compounds crystallize in a monoclinic unit cell and adopt a "layer-by-layer" organization with the molecules in each layer packed in a herringbone motif. However, subtle differences in packing features of the three compounds are evident from the Hirshfeld surfaces (Fig. 2a) and their relative 2D fingerprints (Fig. 2b) as calculated using the program Crystal Explorer (Version 3.1) [23]. The dominant intermolecular interactions is the C—H … π hydrogen bonds which is manifested as C···H contacts contributing to 22.9–24.3% to their corresponding Hirshfeld surfaces (Fig. 2c). In the fingerprint plots of the two independent molecules of di(Me)$_2$Pr-BTBT these appear as a pair of wings of almost equal lengths in the ($d_i$, $d_e$) regions (1.7 Å, 1.1 Å) and (1.1 Å, 1.7 Å). It must be noted the herringbone packing is stabilized by C—H … π interactions as has been observed in other BTBT derivatives [6,14,29]. The contributions of the S/C···S/C type contacts, corresponding to π … π interactions, are observed to decrease as a function of the bulkiness of the terminal substitution. The combined contribution of these contacts are 10.9% in diiPr-BTBT, 7.8% in ditBuBTBT and, only 1.3 and 1.4% for the two molecules of di(Me)$_2$Pr-BTBT. This is compensated by the increase in the contribution of S···H contacts corresponding to C—H···S interactions from 7.5% in diiPr-BTBT to 15.7% in di(Me)$_2$Pr-BTBT. Thus, the increase in bulkiness decreases the role of π … π interactions in the crystal packing whereas the C—H … π/S type interactions

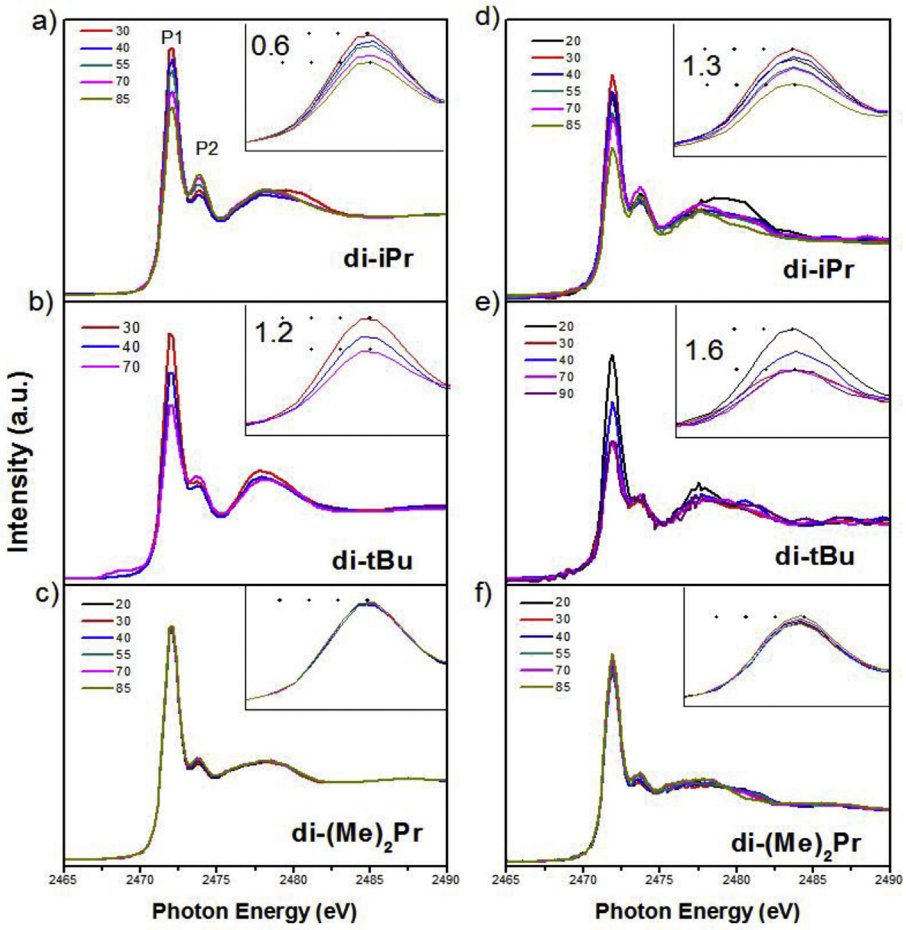


**Fig. 3.** Angle dependent sulfur K-edge NEXAFS spectra for diiPr-BTBT, ditBu-BTBT and di(Me)$_2$Pr-BTBT films deposited on FTO. Angular dependence for the main peak is highlighted in the inset. Comparison of a simultaneous measurement of TEY (left) and FY (right) NEXAFS.

stabilizes the 2D herringbone motif.

With the aim of getting information about the unoccupied electronic structure and film ordering, S 1s NEXAFS spectra were measured by varying the incident angle of the synchrotron radiation (SR) from 20° (grazing incidence) up to 90° (normal incidence) for diiPr-BTBT, ditBu-BTBT, and di(Me)$_2$Pr-BTBT oligomers, as shown in Fig. 3. The spectra are characterized by two peaks (P1 and P2), and a broad band above the ionization potential. Feature P1 may be associated to transitions of core excitation from sulfur 1s electron to π* and σ*(C−S) orbitals, following the assignment of previous angle-dependent NEXAFS studies on thiophene-based polymers [1,2,16,17]. According to these studies, S1s → σ*(C−S) transition is more energetic and intense than S1s → π*, the difference between them is less than 1 eV [17]. The resonant Auger decay results which will be presented next corroborate with these assignments. Feature P2 can be assigned to another S1s → σ*(C−S) transition, however its transition moment is perpendicular to the molecular plane [29]. For diiPr-BTBT and ditBu-BTBT molecules the P1 signal increases with the decrease of the SR incident angle, reaching a maximum value at θ = 20° (or 30°). Feature P2 shows clearly the opposite behavior. This is well explained by the fact that the maximum intensity for any resonance will be expected when the direction of the electric field vector of the synchrotron light is parallel to the molecular orbital. A stronger dichroism is present for the ditBu-BTBT oligomer (Fig. 3b and e), characteristic of a well-ordered film. The polarization dependence of the intensities of the NEXAFS spectra is also observed for the diiPr-BTBT film (Fig. 3a and d), but it is less prominent than for the ditBu-BTBT film. In both cases the preferred molecular orientation is that with the molecular plane perpendicular to substrate surface, by considering the opposite behavior of the P1 and P2 NEXAFS features with the angle of the incident radiation. The angle formed between the oligomer backbone and the substrate (tilt angle) could not be determined and certain inclination of the molecular plane cannot be ruled out, and indeed it is expected as XRD measurements demonstrated [6]. For the di(Me)$_2$Pr-BTBT film (Fig. 3c and f) no angular variation (no dichroism) is seen. This could let us to suggest that we were dealing with an essentially disordered film. However, crystal structure determination for this oligomer showed that it packs in a herringbone motif, for which films NEXAFS spectra would respond equally. This lead to the conclusion that we have grown films which maintained its crystal structure. Indeed all oligomers under investigation pack in a herringbone structure but nevertheless the crystal structure of di(Me)$_2$Pr-BTBT is very different from those of diiPr-BTBT and ditBu-BTBT. The relative distances and positions of the aromatic cores vary considerably between di(Me)$_2$Pr-BTBT and diiPr-BTBT/ditBu-BTBT (see Fig. 1), which may explain the different dichroism responses.

The different degree of ordering at the surface and in the bulk of the oligomer films was evaluated by comparing spectra measured by TEY and FY NEXAFS. The difference in intensity of peak P1 between normal and grazing incidence of the incoming light is 1.3 and 1.6 (Fig. 3d and e) in the bulk of diiPr-BTBT and ditBu-BTBT films, respectively. These values are much greater than those observed for surface-sensitive NEXAFS spectra of diiPr-BTBT (0.6) and ditBu-BTBT (1.2) films (Fig. 3a and b), reflecting a less organization of the films at the surface. Furthermore, the bulk of the ditBu-BTBT oligomer tends to be more ordered in comparison with the diiPr-BTBT molecule. In all cases the variation in the intensities are much more pronounced in the bulk of the

materials, suggesting that the ordering of the films is greater in the bulk than at the surface. The preferred molecular orientation of diiPr-BTBT and ditBu-BTBT films is the same at the surface as well as in the bulk: edge-on geometry of the organic backbone. For materials to be used in field effect transistors an upright position of the molecular plane would be the desired geometry, facilitating the source-drain current through the π overlap [30].

X-ray absorption spectra of diiPr-BTBT, ditBu-BTBT, and di(Me)$_2$Pr-BTBT films deposited on Si and ITO substrates were measured additionally (Figures S7 and S8, respectively). On silicon it seems that the substrate doesn't interfere much in film formation, which presents similar trends at the surface and in the bulk. Again di(Me)$_2$Pr-BTBT films show approximately no angular dependence. Although the preferred molecular orientation is also maintained on ITO, some differences emerges: stronger dichroism for the ditBu-BTBT at the surface, little variation between surface and bulk is seen for diiPr-BTBT films and angular dependency for di(Me)$_2$Pr-BTBT spectra especially in the bulk. These results indicate that the preferred edge-on molecular orientation is preserved even by varying the nature of the substrate surfaces.

Resonant Auger Spectroscopy (RAS) in conjunction with the core-hole-clock approach was used to study the influence of different substituents in the [1]benzothieno [3,2-b]benzothiophene structure on the charge transfer dynamics [31]. When an electron from sulfur 1s is excited into an unoccupied molecular orbital, the system will undergo competitive relaxation processes. The non-radiative process (Auger decay) will be the focus of interest of this work. If the excited electron at the unoccupied molecular orbital is transferred, e.g. to the substrate before the core hole is filled, the final state will be the same as the normal Auger process after ionization. It will be called normal Auger, characterized by constant kinetic energy. On the other hand, if the excited electron still remains as a spectator after the core-hole had been refilled and the Auger electron emitted, peaks referred to the spectator Auger process are observed in the spectra [31–34]. In comparison with the normal Auger peak the spectator peaks appears at higher kinetic energy values, owing to the screening of the core-hole [35].

Fig. 4 shows sulfur $KL_{2,3}L_{2,3}$ Auger decay spectra obtained for the diiPr-BTBT and ditBu-BTBT films, measured at the energy of the first NEXAFS resonance. Three Auger features at different kinetic energies are easily distinguishable. The peak identified by the green line is associated with the emission of the normal Auger electron. The other two peaks are associated with spectator Auger decay channels derived from the S1s → π* (yellow line) and S → σ*(S−C) (blue line) transitions, respectively. According to previous reports, similar structures were attributed [1,2,16,17,36].

**Table 1**
Electronic charge transfer times ($\tau_{CT}$) for diiPr-BTBT and ditBu-BTBT oligomers.

| Photon Enegy (eV) | $\tau_{CT}$ (fs) | |
|---|---|---|
| | diiPr-BTBT | ditBu-BTBT |
| On resonance | 12.12 | 11.57 |

Through the well-established relationship between the intensities of the deconvoluted peaks of the RAS spectrum and the core-hole lifetime (S 1s, $\tau_{CH}$ = 1.27 fs) [30], it is possible to calculate charge transfer times ($\tau_{CT}$) [31]. Table 1 reports charge transfer times for the diiPr-BTBT and ditBu-BTBT oligomers. This result may be associated with the oligomer organization and ordering. The molecular orientation of the oligomers has direct influence in the charge transport process in the films, as already demonstrated for semiconducting polymers and co-polymers containing the thiophene unit [1,2,16,17,30]. DitBu-BTBT and diiPr-BTBT films have preference to acquire a standing-up configuration. This configuration facilitates the efficiency of the charge transport process, decreasing the $\tau_{CT}$ owing to better overlap of π orbitals [35]. For the di(Me)$_2$Pr-BTBT oligomer it was not possible to observe the normal Auger peak in its RAS spectrum (not shown). For this oligomer the electron transfer process may be very slow to be probed by the core-hole clock methodology.

## 4. Conclusions

We have evaluated the influence of the substitution of different alkyl groups in the [1]benzothieno [3,2-b]benzothiophene core on the ordering, molecular orientation and charge delocalization dynamics of oligomers films deposited on different substrate surfaces. The morphology of the films at the surface and in the bulk was investigated by

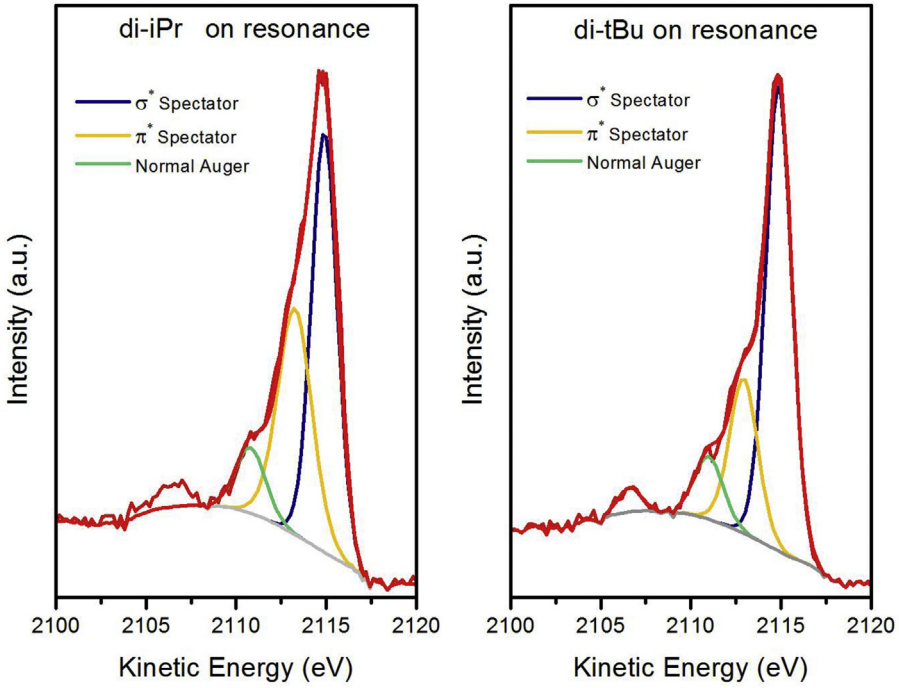


**Fig. 4.** Sulfur $KL_{2,3}L_{2,3}$ Auger decay spectra obtained on resonance for the diiPr-BTBT and ditBu-BTBT films.

TEY and FY NEXAFS spectroscopy, respectively, while ultrafast molecular dynamics were studied by the core-hole clock method. Almost no dichroism was observed for both NEXAFS detection modes for di $(Me)_2$Pr-BTBT film, indicating that the films follow the herringbone crystal packing. From the angular dependence obtained for the diiPr-BTBT film at the sulfur K-edge NEXAFS, we concluded that this molecule tends to form films with some degree of order and in an up-right orientation. The more pronounced dichroism was observed for the ditBu-BTBT film, with similar orientation. In all cases studied greater ordering is observed in the bulk, except for ditBu-BTBT on ITO. The preferable molecular orientation remains the same for all substrates investigated. Shorter charge transfer time was obtained for the ditBu-BTBT film. Combining surface- and bulk-sensitive NEXAFS and RAS results, we deduce that the more efficient process of ultrafast electron transfer takes place at the resonance of the well-organized ditBu-BTBT film.

## Acknowledgments

Research partially supported by LNLS–National Synchrotron Light Laboratory, Brazil. Special thanks to CAPES and CNPq for financial support. The authors acknowledge support from the Walloon Region (WCS Project No 1117306) and from the Belgian National Fund for Scientific Research (FNRS – PDR T.0058.14). B. C. kindly acknowledges support from the F.R.S. - FNRS (Belgian National Scientific Research Fund) for the POLYGRAD Project 22333186. B. C. is a FRS-FNRS Research Fellow.

## Appendix A. Supplementary data

Supplementary data to this article can be found online at https://doi.org/10.1016/j.matchemphys.2018.09.064.

## References

[1] Y. Garcia-Basabe, N.A.D. Yamamoto, L.S. Roman, M.L.M. Rocco, Phys. Chem. Chem. Phys. 17 (2015) 11244.
[2] Y. Garcia-Basabe, C.F.N. Marchiori, B.G.A.L. Borges, N.A.D. Yamamoto, A.G. Macedo, M. Koehler, L.S. Roman, M.L.M. Rocco, J. Appl. Phys. 115 (2014) 134901.
[3] R. Onoki, G. Yoshikawa, Y. Tsuruma, S. Ikeda, K. Saiki, K. Ueno, Langmuir 24 (2008) 11605.
[4] H. Choi, J.S. Park, E. Jeong, G.H. Kim, B.R. Lee, S.O. Kim, M.H. Song, H.Y. Woo, J.Y. Kim, Adv. Mater. 23 (2011) 2759.
[5] Z. Hu, F. Huang, Y. Cao, Small Methods 1 (2017) 1700264.
[6] G. Schweicher, V. Lemaur, C. Niebel, C. Ruzié, Y. Diao, O. Goto, W.-Y. Lee, Y. Kim, J.-B. Arlin, J. Karpinska, A.R. Kennedy, S.R. Parkin, Y. Olivier, S.C.B. Mannsfeld, J. Cornil, Y.H. Geerts, Z. Bao, Adv. Mater. 27 (2015) 3066.
[7] T. Kazuo, Y. Tatsuya, E. Hideaki, I. Takafumi, Sci. Technol. Adv. Mater. 8 (2007) 273.
[8] R. Janneck, N. Pilet, S.P. Bommanaboyena, B. Watts, P. Heremans, J. Genoe, C. Rolin, Adv. Mater. 29 (2017) 1703864.
[9] K. Haase, C. Teixeira da Rocha, C. Hauenstein, Y. Zheng, M. Hambsch, S.C.B. Mannsfeld, Advanced Electronic Materials 4 (2018) 1800076.
[10] G. Schweicher, Y. Olivier, V. Lemaur, Y.H. Geerts, Isr. J. Chem. 54 (2014) 595.
[11] A. Pérez-Rodríguez, I. Temiño, C. Ocal, M. Mas-Torrent, E. Barrena, ACS Appl. Mater. Interfaces 10 (2018) 7296.
[12] T. Okamoto, C. Mitsui, M. Yamagishi, K. Nakahara, J. Soeda, Y. Hirose, K. Miwa, H. Sato, A. Yamano, T. Matsushita, T. Uemura, J. Takeya, Adv. Mater. 25 (2013) 6392.
[13] C. Reese, M.E. Roberts, S.R. Parkin, Z. Bao, Adv. Mater. 21 (2009) 3678.
[14] Y. Tsutsui, G. Schweicher, B. Chattopadhyay, T. Sakurai, J.B. Arlin, C. Ruzie, A. Aliev, A. Ciesielski, S. Colella, A.R. Kennedy, V. Lemaur, Y. Olivier, R. Hadji, L. Sanguinet, F. Castet, S. Osella, D. Dudenko, D. Beljonne, J. Cornil, P. Samori, S. Seki, Y.H. Geerts, Adv. Mater. 28 (2016) 7106.
[15] G.H. Roche, D. Thuau, P. Valvin, S. Clevers, T. Tjoutis, S. Chambon, D. Flot, Y.H. Geerts, J.J.E. Moreau, G. Wantz, O.J. Dautel, Advanced Electronic Materials 3 (2017) 1700218.
[16] Y. Garcia-Basabe, B.G.A.L. Borges, D.C. Silva, A.G. Macedo, L. Micaroni, L.S. Roman, M.L.M. Rocco, Org. Electron. 14 (2013) 2980.
[17] B.G.A.L. Borges, A.G. Veiga, L. Tzounis, A. Laskarakis, S. Logothetidis, M.L.M. Rocco, J. Phys. Chem. C 120 (2016) 25078.
[18] U. Aygül, D. Batchelor, U. Dettinger, S. Yilmaz, S. Allard, U. Scherf, H. Peisert, T. Chassé, J. Phys. Chem. C 116 (2012) 4870.
[19] M.B. Casu, B.-E. Schuster, I. Biswas, C. Raisch, H. Marchetto, T. Schmidt, T. Chassé, Adv. Mater. 22 (2010) 3740.
[20] J. Stöhr, NEXAFS Spectroscopy, Springer, Germany, 1992.
[21] C.F.N. Marchiori, Y. Garcia-Basabe, F. de A. Ribeiro, M. Koehler, L.S. Roman, M.L.M. Rocco, Spectrochim. Acta Mol. Biomol. Spectrosc. 171 (2017) 376.
[22] U. Aygül, H. Peisert, D. Batchelor, U. Dettinger, M. Ivanovic, A. Tournebize, S. Mangold, M. Förster, I. Dumsch, S. Kowalski, S. Allard, U. Scherf, T. Chassé, Sol. Energy Mater. Sol. Cell. 128 (2014) 119.
[23] D.J.G.S.K. Wolff, J.J. McKinnon, M.J. Turner, D. Jayatilaka, M. Spackman, A.Crystal Explorer 3.1, University of Western Australia, Crawley, Australia, 2012.
[24] R.C.M. Salles, L.H. Coutinho, A.G. da Veiga, M.M. Sant'Anna, G.G.B. de Souza, J. Chem. Phys. 148 (2018) 045107.
[25] Y. Garcia-Basabe, A.R. Rocha, F.C. Vicentin, C.E.P. Villegas, R. Nascimento, E.C. Romani, E.C. de Oliveira, G.J.M. Fechine, S. Li, G. Eda, D.G. Larrude, Phys. Chem. Chem. Phys. : Phys. Chem. Chem. Phys. 19 (2017) 29954.
[26] E. Carrasco, M. Oujja, M. Sanz, J.F. Marco, M. Castillejo, Microchem. J. 137 (2018) 381.
[27] A. Batra, G. Kladnik, H. Vázquez, J.S. Meisner, L. Floreano, C. Nuckolls, D. Cvetko, A. Morgante, L. Venkataraman, Nat. Commun. 3 (2012) 1086.
[28] H. Hintz, H. Peisert, U. Aygul, F. Latteyer, I. Biswas, P. Nagel, M. Merz, S. Schuppler, D. Breusov, S. Allard, U. Scherf, T. Chasse, ChemPhysChem : Eur. J. Chem. Phys. Physical Chem. 11 (2010) 269.
[29] I.-S. Hiromi, S. Tetsuhiro, Jpn. J. Appl. Phys. 53 (2014) 02BB07.
[30] Y. Garcia-Basabe, C.F.N. Marchiori, C.E.V. de Moura, A.B. Rocha, L.S. Roman, M.L.M. Rocco, J. Phys. Chem. C 118 (2014) 23863.
[31] D. Menzel, Chem. Soc. Rev. 37 (2008) 2212.
[32] A. Föhlisch, P. Feulner, F. Hennies, A. Fink, D. Menzel, D. Sánchez-Portal, P. M Echenique, W. Wurth, Nature 436 (2005) 373.
[33] L. Cao, X.-Y. Gao, A.T.S. Wee, D.-C. Qi, Adv. Mater. 26 (2014) 7880.
[34] W. Wurth, D. Menzel, Chem. Phys. 251 (2000) 141.
[35] W. Chen, D.-C. Qi, H. Huang, X. Gao, A.T.S. Wee, Adv. Funct. Mater. 21 (2011) 410.
[36] H. Ikeura-Sekiguchi, T. Sekiguchi, Surf. Interface Anal. 40 (2008) 673.